Brain-heart dynamics in emotional processing under uncertainty index depression risk

Hui-Ling Chan[1], Noriaki Kanayama[2,3], Ryohei Mizuochi[4], Shigeto Yamawaki[5], Maro G. Machizawa[6]

[1] Center for Brain, Mind and KANSEI Sciences Research, Hiroshima University, Hiroshima 734-8551, Japan. Tel: +81–82–257–1722. E-mail: chanhl@hiroshima-u.ac.jp

[2] National Institute of Advanced Industrial Science and Technology, Ibaraki 305-8566, Japan. Tel: +81–29–861–8167. E-mail: kanayama.n@aist.go.jp

[3] Center for Brain, Mind and KANSEI Sciences Research, Hiroshima University, Hiroshima 734-8551, Japan.

[4] Center for Brain, Mind and KANSEI Sciences Research, Hiroshima University, Hiroshima 734-8551, Japan. Tel: +81–82–257–1722. E-mail: rmizu349@hiroshima-u.ac.jp.

[5] Center for Brain, Mind and KANSEI Sciences Research, Hiroshima University, Hiroshima 734-8551, Japan. Tel: +81–82–257–1722. E-mail: yamawaki@hiroshima-u.ac.jp

[6] Center for Brain, Mind and KANSEI Sciences Research, Hiroshima University, Tokyo 130-0003, Japan. Tel: +81–50–8880–8806. E-mail: machizawa@hiroshima-u.ac.jp

- Corresponding author:

Hui-Ling Chan (chanhl@hiroshima-u.ac.jp)

Abstract

Recent studies highlight interoception as essential to processing healthy emotion and to pathology of major depressive disorder. However, it is unclear how individual differences in healthy people with high depression risk (HDR) relate to neurophysiological underpinnings for interoception and emotional reactions under different degrees of certainty. We examined whether the degree of depression risk mediates the relationship between heartbeat-evoked potential (HEP) as a neurophysiological marker for cardiac interoception and heart rate (HR) or heart rate variability (HRV) as indices for cardiac reactivity. In a concurrent EEG-ECG experiment, 26 healthy participants underwent an emotion-evoking picture-evaluation task. Each of differential auditory cues was associated with certainty of the upcoming pleasant or unpleasant picture. The results showed that HDR reduced neural sources in anticipation and enhanced physiological reactions to uncertain, unpleasant pictures. These results suggest that weak predictions and augmented prediction errors for negative emotional stimuli reflect depression risk. Moreover, depression risk significantly mediated the relationship between HEP and HR for unexpected unpleasant stimuli. Strong association between brain and heart reactivity was observed in HDR individuals, suggesting a potential involvement of alternations in baroreflex sensitivity. This study provides evidence that interoception and autonomic regulation in the cardiac domain is altered by depression risk and highlights that specific component of brain-heart interactions would offer insights into the underlying mechanism of autonomic nerve system and interoception disturbances associated with depression risk.

1. Introduction

Emotions are affected by an external or internal events and are governed by the intrinsic force to maintain the current emotional state (1). Among various types of emotion, depression, or an emotional state marked by a constantly low mood, is characterized by an alternation of emotional processing. Accumulating evidence suggests that interoception, the perception of bodily states, is a key to understanding emotional processing and the pathology of major depressive disorder (MDD) (2). Behavioral (3) and neuroimaging (4) studies of MDD patients have reported impaired interoceptive functions in MDD. In depression, while neural mechanisms implicated in the interaction between interoception and emotional processing have been extensively explored to date (5), investigations on the relationship between interoception and autonomic regulation responding to emotional content have just begun.

Our cardiac autonomic systems automatically respond to emotional events. For example, heart rate (HR) (6) and heart rate variability (HRV) (7) are well-known markers for cardiac reactivity that reflect changes in valence (pleasant or unpleasant emotional states). Heartbeat-evoked potentials (HEPs) on the other hand represent *neural* responses for each heartbeat and thought to reflect interoceptive cardiac processing in the brain (8). It has been suggested that generation of HEPs may reflect a projection of cardiac *afferent* signals from the heart to brain regions, such as the insula, where interoception is signaled from the vagus nerve and brainstem (9). Studies of brain-heart interactions have also reported that HEPs (10), the coupling of brain theta activity and cardiac activity (11), and the correlation between HEP and HRV (12) were modulated by emotion. Therefore, HEP and HR/HRV are putatively great candidates for quantitative neuro-cardiac substrates for psychological/psychiatric risks.

An increasing body of research suggests a link of MDD to impaired interoceptive system (13). Individuals with ‘high depression risk (HDR)’ who have elevated risks of developing MDD (14) also show altered interoception, such as reduced connectivity in the brain interoceptive network (15, 16). Thus, alterations in the interoceptive system may span the entire spectrum, along with the depressive trait. As a measure of interoception, HEP amplitudes have been found reduced in MDD patients during resting state (17). Moreover, the interoceptive system is responsible for regulatory processes to maintain or restore homeostatic balance at both conscious and autonomic levels (18, 19). It has been also found strong relations between HEP and cardiac regulation functions such that alternations of HEP were related to

autonomic symptoms (20) and that HRV neurofeedback training revealed converse correlation between HRV and HEP compared to emotional conditions (12). Moreover, HDR individuals had reduced HR recovery rate in response to unpleasant images (21) and reduced HRV during resting state (22). Alterations of cardiac autonomic regulation may affect interoceptive cardiac system, so-called brain-heart communications. While literature has suggested depression link to dysfunction of interoceptive system and altered cardiac reactivity, it is currently unknown whether variances in depression risk would mediate the association between interoceptive cardiac system and cardiac activity.

The disturbance of interoception in MDD may be associated with an inefficient internal model and unreliable prediction errors (23). According to predictive coding theory (24-26), the brain constantly predicts future sensory inputs and updates the internal model to improve prediction (perceptual inference) or acts based on the prediction errors (active inference). The brain interoceptive network (BIN) processes prediction error signals ascended from visceral organs via brainstem, and then generates prediction signals to modulate visceral activity via autonomic nerve system (ANS). As a part of the homeostatic function, the body auto-regulates even before the anticipatory event so as to minimize the prediction error (27). At the neural level, preparatory activity related to prediction formation is known, such that neurons fire even before the incoming sensory inputs (28, 29). It has also been proposed that cardiac regulation plays a role to maintain homeostatic state of mind by reducing surprise against uncertainty (30). Previous studies have shown that compared to certain conditions, *uncertainty* induced greater regulatory responses in both cardiac (31, 32) and neuro-cardiac (33, 34) reactivity, which may result from large prediction errors. Moreover, abnormal anticipation of future events has been observed from the central interoceptive system in individuals with HDR (35, 36). However, it is yet unclear whether activity of the interoceptive cardiac system and cardiac reactivity for certainty and uncertainty reflect individual differences in depression risk.

The present study investigated neural substrates of interoceptive cardiac system and cardiac reactivity under certainty and uncertainty in healthy individuals. Both electroencephalograms (EEG) and electrocardiograms (ECG) were monitored while participants performed an emotion-evoking picture-evaluation task. The pre-cue tone was played to induce anticipatory responses, followed by a display of either a pleasant or an unpleasant image. As an index of neuro-physiological interaction, HEP was assessed, and HR and HRV were assessed as indices of cardiac reactivity. Based on previous literature on cardiac

reactivity, we used predictive coding theory to hypothesize that stimuli with *negative* valence (unpleasant pictures) under *uncertainty* would elicit larger responses. A mediation analysis was performed to further examine the role of depression risk in cardiac regulation, specifically the interactions between neural subtracts and physiological reactivity. Since little is known about spatiotemporal dynamics of HEP, Finally, given an assumption that HEP may not be a solitary component, we further examined which specific time and spatial feature of HEP plays a pivotal role in the mediation among the trilogy in a data-driven manner. Altogether, we examined how cardiac and neurophysiological signals interact with interoceptive prediction and prediction errors in association with depression risk.

2. Materials and Methods

2.1. Participants

Twenty-six healthy participants (16 females; mean and standard deviation (*SD*) of age: 22.19 ± 1.86 years old) with no history of psychiatric, psychological, or cardiac disorders, participated in concurrent EEG-ECG recording during an emotion-evoking picture-evaluation task. Data were acquired from a previous study (37).

2.2. Questionnaire procedure

The level of depression risk was evaluated using the Japanese version of Beck Depression Inventory-II (38, 39). The overall mean and *SD* of the BDI score were 5.65 ± 7.22. Extreme groups approaches are suitable for analysis and visualization of skewed data or data with small sample size (40) and avoid misclassification of samples at around the median scores (41). In this study, for display purposes for some data analyses, participants were split into two groups using quartile split (42). Participants having BDI scores higher than the third quartile (BDI $\geq$ 5) and lower than the first quartile (BDI $\leq$ 2) were categorized into high BDI (n = 8, BDI = 14.12 ± 7.42) and low BDI (n = 13, BDI = 1.23 ± 0.89) groups, respectively.

2.3. Behavioral task and procedure

The emotion-evoking picture-evaluation experiment consisted of 240 trials. Each trial was comprised of a pre-cue and a picture-presentation phases followed by a subjective evaluation of valence. During the pre-cue (‘cue’ phase), an auditory tone was presented for 0.25 s, followed by a 3.75-s blank period. During a picture-presentation (‘pic’ phase), either a pleasant or an unpleasant picture was displayed for 4 s, in which

participants were asked to evaluate the emotion they felt. Participants rated their emotional valence on a four-point Likert scale (from most unpleasant to most pleasant) immediately after seeing a picture during the evaluation phase. Three different tones (low, mid, and high at 500, 1000, and 1500 Hz, respectively) were used as auditory pre-cues to indicate three predictive conditions: predictable pleasant (PP), predictable unpleasant (PU), and unpredictable (UX). The unpredictable condition contained two conditions based on the valence of the picture actually shown: unpredictable pleasant (UP) and unpredictable unpleasant (UU). Note that we abbreviate the conditions in this manuscript as follows: the letter X indicates the combination of possible conditions. For example, UX represents a combination of UP and UU conditions (unpredictable conditions regardless of the subsequent valence of the picture), whereas XU represents a mixture of PU and UU conditions (negative picture conditions regardless of the tone). The mid (1000-Hz) tone was the cue for the UX condition. The 500- and 1500-Hz tones were used in either PP or PU conditions (the assignment was counterbalanced across participants). Each of the three predictive conditions consisted of 80 trials. In the UX condition, 40 trials showed pleasant pictures (UP) and another 40 showed unpleasant pictures (UU). Pictures were selected from the International Emotional Picture System (IAPS) (43). Finally, participants rated their emotions after seeing the images. For further details, please refer to Machizawa, Lisi, Kanayama, Mizuochi, Makita, Sasaoka and Yamawaki (37).

2.4. EEG-ECG simultaneous recordings

During the task, brain and cardiac activity were simultaneously recorded using the BioSemi ActiveTwo system (BioSemi, Amsterdam) at a sampling rate of 2,048 Hz. The 64-channel EEG electrodes were placed according to the conventional international 10-20 montage. In addition to EEG channels, ECG electrodes were placed on the left wrist and right side of the back of the neck to monitor bipolar ECG signals. Additionally, a conventional bipolar electrooculography (EOG) was monitored to measure vertical and horizontal eye movements. Four EOG electrodes were individually placed above and below the right eye and left and right of the outer canthi. An additional channel was placed at the tip of the nose for offline re-reference.

2.5. HR and HRV computation

Preprocessing and R peak detection from ECG signals were conducted using the Python package, BioSPPy (44). Raw ECG signals were first bandpass-filtered with an FIR filter with a passband frequency range of

3–45 Hz, followed by detection (45) and location correction of R peaks by relocating each R peak to the time point with the maximum ECG signal within the time range of –50 to 50 ms.

Instantaneous heart rate (HR) was computed from the inverse of the inter-beat interval (IBI) between two successive R peaks. For subsequent analyses, instantaneous HR data points exceeding the physiological range (40–200 bpm) were discarded. Finally, time series of HR were obtained by applying boxcar smoothing with a window size of 3 and cubic spline interpolation to those instantaneous HRs.

As an HRV index, we employed *SD* of normal-to-normal IBI (SDNN) in the current study (46-48). To obtain the time series of HRV, IBIs with z-scores larger than 1.96 were discarded and then the remaining IBIs were up-sampled to 4 Hz using cubic spline interpolation. Then a 10-s sliding window with a 0.25-s step was applied to the interpolated IBIs to compute the *SD* of IBIs within the window as the instantaneous HRV value at the center of the window. The resulting 4-Hz time series of HRV was further up-sampled to the original sampling rate of EEG at 2,048 Hz to match the sampling rate. We set the following rejection criteria to assure the quality of HR and HRV indices. Epochs of HR and HRV were extracted between 1 s before and 20 s after cue display onset. For each participant, two types of outliers were detected across and within trials and discarded according to robust z-score criteria: (1) *epochs* with absolute robust z-scores larger than a threshold of 3.4807 (equivalent to $p = .0005$) after applying a robust z transform to mean values of all epochs, and (2) epochs with robust z-scores of any *sample* larger than the threshold after applying a robust z transform to the time series within the same epoch. These cleaned data were employed in subsequent analyses. The remaining epochs of HR and HRV were downsampled to 200 Hz and averaged across epochs of the same condition within participants for subsequent analysis.

2.6. HEP computation

EEG signals were preprocessed using EEGLAB toolbox v2019.1 for Matlab (49). Continuous raw data were bandpass-filtered (1–40 Hz), downsampled to 256 Hz, epoched to cue-onset (–1 s to 10 s), and baseline-corrected (–1 s to 0 s). Artifactual epochs were detected by the automatic rejection algorithm implemented in EEGLAB. Eye-related artifacts were corrected using automatic EOG correction with conventional recursive least squares regression. An extended Infomax-independent component analysis was performed to remove EOG- and ECG-related components. Noise-free epochs were then re-referenced

to the average reference of EEG signals. Finally, 9.55% of EEG epochs were discarded and 217±14.82 epochs per participant were remained.

For each of the EEG epochs, the time of R peaks was detected from corresponding bandpass-filtered ECG signals for two periods 0.5–3.4 s after cue-onset (within the cue phase) and 4.5–7.4 s after cue-onset (equivalent to 0.5–3.4 s after picture-onset; during the pic phase). In this study, the R peaks close to cue and picture presentations were not applied to HEP computation in order to minimize direct perceptual effects of auditory and visual stimuli, respectively.

EEG-ECG epochs containing falsely detected R peaks were detected and discarded based on careful visual inspection. On average, 2.46±9.50 EEG-ECG epochs were discarded and 214.62±15.60 EEG-ECG epochs were remained. For retained EEG-ECG epochs, time points of R peaks were used as the onset time to further epoch EEG signals (–0.1 to 0.6 s), followed by baseline correction (–0.1 to –0.05 s). The duration of baseline correction was ended at 0.05 s before R peaks to avoid cardiac artifacts. The HEPs were then computed for corresponding conditions during the cue phase (PP_cue, PU_cue, UP_cue, and UU_cue) and pic phase (PP_pic, PU_pic, UP_pic, and UU_pic) separately. The number of HEP epochs was 241.77±37.91 for each of four predictable conditions (PP_cue, PP_pic, PU_cue, and PU_pic) and 120.71±19.86 for each of four unpredictable conditions (UP_cue, UP_pic, UU_cue, and UU_pic). Note that onset times of HEP signals were the time points of R peaks, as per convention, while that of cardiac reactivity was the time of cue display onset.

To identify morphology of HEPs, surrogate HEPs were computed based on surrogate R-peaks that were randomly jittered in a range of –0.1 to 0.1 s from the time points of real R peaks (33). HEPs and surrogate HEPs of each participant were then individually averaged across all epochs regardless of condition. A nonparametric cluster-level F-test for spatiotemporal data implemented in MNE-Python (50) was then applied to the averaged HEP and averaged surrogate HEP waveforms to identify clusters of channels and time periods revealing significant neural responses to heartbeats within the time-window of 0.1 to 0.6 s after the R-peak onset. Any electrodes located within 5 cm of each other were considered spatial neighbors. The number of permutations was set to 2,500 and the threshold to form clusters was an F-value corresponding to an uncorrected *p*-value of .00001.

2.7. Statistical analysis

In this study, computations of repeated-measures ANOVA (RM-ANOVA), correlation, and mediation analysis were performed using Python package pingouin (51). Computations of *t*-tests, and FDR correction were performed using implementations in the Python packages, SciPy (52) and statsmodels (53), respectively. Our α-level for FDR-corrected *p*-values (p_{FDR}) was set at 0.05. As necessary, uncorrected *p*-values ($p_{\mathrm{uncorrected}}$) less than 0.05 were also reported to show the trend for completeness. Note that the correlation analysis in this study indicates partial correlation controlled for age and sex, which have been shown to affect emotional processing (54-58), HEP (59), and cardiac activity (60). Effect sizes of partial correlation were measured using r^2.

2.7.1. Cardiac reactivity modulated by depression risk

To examine whether depression risk altered cardiac reactivity in response to cues and emotional pictures, the interrelationship between cardiac reactivity and BDI was computed for each condition, PP, PU, UP, and UU. Firstly, periods showing significant main effects of cues or emotional pictures were identified by performing RM-ANOVA on the HR or HRV for each time point, followed by multiple comparison correction using the false discovery rate (FDR). Since recovery duration (waveform returned to baseline) for HR and HRV appeared to differ, we considered different time-windows for HR and HRV: 12 s for HR waveform and 20 s for HRV waveform. For each of the identified significant time periods, the correlation between the temporal averaged cardiac reactivity of each condition and BDI scores was computed, followed by multiple comparison correction using FDR.

We further examined whether individual differences in cardiac reactivity responding to various certainty levels reflected depression risk. The durations showing significant effect of certainty level was first examined via comparing of HR or HRV signals between certain (PP and PU) and uncertain (UP and UU) conditions using paired *t*-tests for each time point. For each of durations showing significant effects of certainty, *certainty effects* were assessed on the temporal average of *differences* between predictable and unpredictable conditions, PP – UP and PU – UU, as the measures of prediction errors in positive and negative emotional conditions, respectively. Since no sample points survived after FDR correction across time, significant time periods during uncorrected *p*-values ($p_{\mathrm{uncorrected}}$) less than 0.05 were reported. Then,

the correlation between certainty effects and BDI scores was computed, followed by multiple comparison correction using FDR.

2.7.2. Interrelationship between depression risk, cardiac reactivity, and HEP

For those conditions showing significant effects of depression risk on cardiac reactivity or certainty differences, the interrelationship between the depression risk and the activity of cardiac interoceptive system was further quantified. The correlation between BDI scores and mean HEP amplitudes of each of spatiotemporal HEP clusters was computed at each of cue and pic phases. The certainty effects on HEP were analyzed separately in cue and pic phases to represent prediction and prediction error signals in central processing of cardiac signals, respectively. Multiple comparison correction across clusters and phases was performed using FDR.

To show whether the interaction between cardiac interoceptive system and cardiac regulation function was altered with depression risk, mediation analysis was applied to examine the following model: the relationship between the HEP and cardiac reactivity mediated by depression risk, controlled for age and sex. The analysis was performed on the conditions, durations, and clusters showing significant correlation to BDI scores.

2.8. Control analyses

Cardiac activity affects amplitudes of EEG signals and leads to cardiac field artifacts (CFA). Although careful preprocessing on EEG signals was performed to reduce CFA, we additionally analyzed ECG mean amplitudes to address that ECG did not account for the differences of HEP. We obtained ECG epochs from the bandpass-filtered ECG signals epoched using the time points of R peaks as the onset time (–0.1 to 0.6 s), followed by baseline correction (–0.1 to –0.05 s). To test the effect of cues and emotional pictures on the ECG amplitude, RM-ANOVA with post hoc tests was performed for each time point during 0.1–0.6 s, followed by multiple comparison correction using FDR. The RM-ANOVA was also performed on ECG amplitudes of R peaks separately for cue phase and pic phase. Moreover, correlations between BDI scores and the temporal averaged ECG amplitudes was computed for each of the time windows corresponding to HEP spatiotemporal clusters. The correlations between BDI and amplitudes of R peaks and between BDI and certainty effects on amplitudes of R peaks were also performed for each condition.

2.9. Correlation between HR and HRV

Previous studies have shown that HR and HRV were negatively correlated (61, 62). Even when the correlation was found, interactions between cardiac activity and tasks or subject groups were found to be distinct when using various cardiac measures (63). Most of previous HR and HRV studies computed averaged values from the whole epochs. However, our analysis was performed on the time series of HR and HRV to identify the time windows showing significant effects. To examine the feasibility of identified time windows, the correlation between the temporal averaged HR and HRV signals was computed for each condition and negative correlation was expected to be observed.

3. Results

3.1. Effect of cues, emotional pictures, and depression risk on HR

In all of the four conditions, HR slightly increased after cue display onset and then decreased (Figure 1a). HR time series were strongly modulated by emotional pictures from 5.4–10.7 s after cue presentation (p_{FDR} < .05 and duration > 1 s in cue × pic RM-ANOVA for the main effect of pic). During this period, unpleasant pictures elicited a larger deceleration of HR than pleasant pictures, especially in the unpredictable condition (UU > UP; p_{FDR} < .05 and duration > 1 s in post hoc analysis for the main effect of pic). In the UU condition, the mean values of HR changes were negatively correlated with BDI scores (r = –.612, p_{FDR} = .006, r^2 = .374, power = 0.934) (Figure 2a and Table 1). The high BDI group showed a larger deceleration of HR than the low BDI group (Figure 2b). In the other three conditions (PP, PU and UP), no significant correlation between HR changes and BDI scores was observed (Table 1). In the cue × pic RM-ANOVA of HR time series, main effects of cue were not observed (p_{FDR} < .05 and duration > 1 s).

Effects of certainty on time series of HR were prominent during 0.7–4.1 s and 8.9–11.2 s in pleasant picture conditions ($p_{uncorrected}$ < .05 and duration > 1 s in paired t-tests between PP and UP). However, the BDI scores were not correlated to the differences of HR between PP and UP during either of these two time periods (Supplementary Table 1, see https://figshare.com/s/e841139a1cb0fd3438a9). Moreover, the certainty effects on HR time series were not found in unpleasant picture conditions (UP vs. UU).

3.2. Effect of cues, emotional pictures, and depression risk on HRV

HRV increased after cue display onset, exceeded the maximum peak at around 10 s, and then recovered at around 20 s (Figure 1c). HRV time series were strongly modulated by emotional pictures at 14.8–16.1 s ($p_{\text{FDR-corrected}} < .05$ and duration > 1 s in cue × pic RM-ANOVA for the main effect of pic). During this time period, mean of HRV changes was not significantly correlated to BDI scores for any of the four conditions (Supplementary Table 2, see https://figshare.com/s/e60cc3d5a573c8cce631). In the cue × pic RM-ANOVA of HRV time series, main effects of cue were not observed ($p_{\text{FDR}} < .05$ and duration > 1 s).

Effects of certainty on HRV time series were then further examined separately for pleasant picture (PP vs. UP) and unpleasant picture (PU vs. UU) conditions. HRV time series were found significantly different between PP and UP conditions at 9.1–13.7 s (UP > PP; $p_{\text{uncorrected}} < .05$ and duration > 1 s in paired *t*-tests). During this time period, mean values of differences of HRV between PU and UU were correlated to BDI scores ($r = -.479$, $p_{\text{FDR}} = .036$, $r^2 = .229$, power = 0.719) (Figure 2c and Table 2). Healthy individuals with high BDI scores revealed a larger HRV increase in the unpredictable condition (UU > PU) while those with low BDI scores revealed a larger HRV response in the predictable condition (PU > UU) (Figure 2d). However, differences between PP and UP averaged over 9.1–13.7 s were not correlated to BDI scores (Table 2). In sum, certainty levels to the future coming stimulations modulated HRV during 9.1–13.7 s after the onset of cues in positive conditions, but the modulation effect was associated with depression risk in negative conditions.

3.3. Spatiotemporal clusters of HEP

Comparing the grand averages of the original HEP and surrogate HEP time series, the original one appeared to evoke stronger signals than the surrogate one (Figure 3a). In the nonparametric cluster-level test over original HEP and surrogate HEP spatiotemporal data ($p < .05$, duration > 0.1 s, number of channels >= 3), three significant spatiotemporal clusters were observed over (1) the occipital and left temporoparietal regions from 0.10–0.36 s, (2) the central region from 0.10–0.29 s, and (3) the right temporal regions from 0.29–0.33 s (Figure 3b). Cluster 1 showed a positive deflection, while clusters 2 and 3 showed negative deflections.

3.4. Effect of depression risk on HEP cluster

In Section 3.1, we identified that deceleration of HR in the UU condition was correlated with BDI scores. Targeted on UU condition, we further examined the relationship between BDI scores and mean amplitudes of HEP clusters and found that HEP cluster 1 was correlated with the depression risk when processing unpredictive cues (UU_cue, $r = -.48$, $p_{\text{uncorrected}} = .018$, $p_{\text{FDR}} = .036$; see also Figure 4b and Table 3). In the high BDI group, the positive component of HEP cluster 1 in the UU condition increased less compared to the PU condition (Figure 4a). On the other hand, the HEP of the low BDI group showed a larger increase in UU condition than in PU condition.

Section 3.2 demonstrated that certainty effects on HRV in unpleasant picture conditions, PU – UU, were correlated with BDI scores. Thus, we further examined the relationship between BDI scores and certainty effects on HEP in PU – UU conditions. A significant partial correlation between the certainty effect on HEP and BDI scores was found in cluster 1 at cue phase, but it did not survive after FDR correction (PU – UU, $r = .45$, $p_{\text{uncorrected}} = .047$, $p_{\text{FDR}} = .095$; see also Figure 4c and Supplementary Table 3 (https://figshare.com/s/93b5ce3111e07d9845f4)). No significant correlation was found between BDI scores and the certainty effect on HEP in other clusters at either cue or pic phases.

3.5. Interrelationship of HEP and cardiac reactivity mediated by depression risk

In the UU condition, the mean HEP amplitudes at cue phase and mean HR changes both showed a tendency to predict BDI scores (Figure 2a and Figure 4b). Thus, we further examined the mediation effect of BDI scores on the relationship between HEP of cluster 1 and cardiac reactivity in the UU condition. This analysis showed that the indirect effect of mean HEP amplitude on HR changes mediated by depression risk was significant, whereas the direct effect was non-significant (Figure 5a). To visualize the relationship between HR and HEP altered with BDI scores, linear regression lines were separately fitted for low BDI and high BDI groups and showed distinct orientations between these two groups (Figure 5b).

Moreover, the certainty effects on HEP cluster 1 and HRV in unpleasant picture conditions (PU – UU) were both correlated with BDI scores (Figure 2c and Figure 4c). The direct and indirect effects of HEP amplitude differences on HRV differences mediated by BDI scores were both non-significant (Figure 5c). The linear regression lines fitted for low BDI and high BDI groups both showed positive slopes (Figure

5d), indicating that the relationship between HEP and HRV in PU – UU conditions was not altered with BDI scores. Altogether, our results suggest that the depression risk fully explained the association between HEP responses and HR changes, but not HRV changes, in the UU condition.

3.6. Effect of cues, pictures, and depression risk on ECG signals

The RM-ANOVA analysis with factors of cue and emotional pictures did not reveal significant main effects on any time point of ECG epochs during 0.1–0.6 s (Supplementary Figure 1, see https://figshare.com/s/f9a67aeaaa0c3ffc29cc). The paired *t*-tests on ECG time series also did not reveal significant differences between predictable and unpredictable conditions. Moreover, when RM-ANOVA analysis with factors of cue and emotional pictures to ECG amplitudes of R peaks, main effects of cue and picture as well as their interactions were not significant at either cue or pic phases (Supplementary Table 4, see https://figshare.com/s/fdd31626d5bf3b05c8fa). ECG amplitudes at R peaks were also not significantly correlated to BDI scores in any of PP, PU, UP, and UU conditions (Supplementary Table 5, see https://figshare.com/s/5b8054cff759edb39724). Lastly, for those conditions observed BDI-modulated effects on HEP, we examined the correlation of BDI scores and values of ECG amplitudes averaged over the time periods of spatiaotemporal HEPs clusters and none of correlation was significant (UU condition: Supplementary Table 6, see https://figshare.com/s/6df37d7036ad22edb200; PU – UU condition: Supplementary Table 7, see https://figshare.com/s/2d7a99cb7ff827cd1844). Thus, the results of control analysis suggest that the modulation effects observed from HEP amplitudes were not driven by ECG artifacts and may represent modulations on cortical processing of heartbeat signals.

3.7. Non-significant negative correlation between HR and HRV

As expected, the mean values of HR changes were negatively, but not significantly, correlated with HRV changes for the time windows showing significant main effect of emotional picture in RM-ANOVA analyses (HR: 5.4–10.7 s; HRV: 14.8–16.1 s) (Supplementary Figure 2, see https://figshare.com/s/e9da2893489d67e8dc86). Thus, relationships between HR and HRV changes in our selected time windows showed similar tendency with previous studies, suggesting the feasibility of our data-driven approach to select time windows for further analysis.

4. Discussion

This study examined the extent to which depression risk is associated with cardiac and neurophysiological emotional responses in certain and uncertain circumstances. A comprehensive temporal characterization of HR, HRV, and HEP responses revealed dissociable and unique relations between certainty of predictive cues in the low BDI and high BDI groups. These results support the hypothesis that depression risk alters processes for interoceptive predictive coding and increases the fluctuation of physiological responses against unpredictable stimuli. It appears that depression risk influences anticipatory HEP responses and mediates the relationship between the HEP and HR especially responding to UU pictures (unexpectedly confronting a negative picture). Importantly, the above-mentioned HEP findings were not explained by any features in ECG, validating unique role of HEP. These results suggest that individuals with high depression risk reduce neural resources for anticipation and increase prediction errors against unpredictable negative events. The present study offers evidence for the disturbances of ANS and interoception as indicators of high depression risk.

In line with our expectation, modulation effects of BDI were observed from HR, HRV, and HEP signals in negative emotional conditions, not in positive emotional conditions. Correlation between RRI and self-report of valence level has been reported for processing negative valence and was not found for positive valence (64), indicating stronger modulation of cardiac activity for generating negative emotion. Thus, processing of negative valence may rely more on interoceptive information than that of positive valence. Moreover, attentional bias for negative events might be notable characteristics of individuals with MDD (65) and with subclinical depression (66). Therefore, our findings suggest the alterations of ANS and cardiac interoceptive system in HDR individuals, which may be reflected by neural and physiological cardiac responses to negative stimulations.

Altered HEP and cardiac reactivity to unpredictable negative events may be particularly relevant to the model relating dysfunction of interoceptive system and atypical autonomic regulation to risk of depression. Abnormal cardiac activity (67-69) and low interoceptive sensibility (70-72) have been widely documented in depressed patients, suggesting the link of depression to autonomic imbalance and impaired interoceptive system. Our findings extended the knowledge that the disturbances of cardiac autonomic functioning and brain interoceptive network were also observed in healthy individuals with depression symptoms.

Although causality between depression and dysfunction of ANS and interoception system is unconfirmed, some longitudinal evidences suggest that dysfunctions of ANS and interoception may precede the onset of depression. Recently, two longitudinal studies showed the predictive effect of resting-state HRV on subsequent depressive symptoms (69, 73), suggesting that disturbances of ANS may increase depression susceptibility. Somatic symptoms, which have been related to dysfunctions of interoceptive systems, can also predict subsequent depression (74, 75), implying the link between abnormal interoceptive system and high depression risk. The exact mechanisms for how disturbances of ANS and interoception may increase depression risk are still unknown. Disturbances of ANS can elicit inflammation (76) and dysregulation of metabolism (77). Low sensitivity in interoceptive signals may lead to disrupted interoceptive predictive coding processing (23, 78), which is crucial to emotional processing and allostatic regulation.

Moreover, our findings in mediation analysis showed enhanced association between HEP and HR in high BDI individuals under uncertainty conditions (Figure 5a), suggesting enhanced brain-heart interactions in healthy individuals with high depression risk. It is in line with the previous study that enhanced neural control on cardiac activity in subclinical depression during resting state (79). The enhanced association may result from reduced baroreflex sensitivity (BRS), which has been reported in depressed patients (80, 81). BRS can be assessed by the association between R-R intervals and blood pressure (BP), where a steeper line represents higher BRS (82). Baroreflex is one of key mechanisms to maintain homeostasis and reduce fluctuations of BP (83). Decreased BP reduces the activation of baroreceptors and their effects on central inhibitory pathway, leading to increased sympathetic tones, HR, and BP. Minati et al. (84) reported reduced BP and HR during processing of negative emotion. Notably, the trend of HR time series in our study was consistent with results of (84). Moreover, BP responses was found to be correlated to the activation of central feedback pathway arising from baroreceptors in tasks of emotional picture perception (85). Increased variability of BP has been related to increased severity in subthreshold depression, suggesting the link between dysfunction of baroreflex and high depression risk (86). Thus, we speculated that high BDI individuals have reduced BRS. In individuals with low BDI, the changes of HR in response to negative stimuli may be partly contributed from baroreflex. In contrast, for individuals with high BDI, their low BRS may reduce the effect of baroreceptor on brain, leading to enhance brain-heart connections. Dysfunctions of baroreceptor may also explain their exaggerated cardiac reactivity, or low capability to maintain homeostasis. Thus, the strategies for cardiovascular diseases such as cardiac rehabilitation and

exercise training to restore BRS (87-90) may constitute an nonpharmacological intervention to reduce depression risk (91, 92). More investigations on the relationship of baroreflex and depressive symptoms are needed to extend the understanding of mechanisms underlying abnormal autonomic and interoceptive activity.

The low anticipatory HEP observed in high BDI individuals may imply their reduced sensitivity on cardiac afferent signals (Figure 4a–b). Notably, reduced HEP amplitudes have been reported in MDD patients compared to healthy controls (17). In contrast, among healthy participants, HEP amplitudes were not altered with depression level (79, 93). The differences between studies may result from different tasks, used electrodes, and selected time windows. Catrambone, Messerotti Benvenuti, Gentili and Valenza (79) compared HEP amplitudes averaged over 250 to 500 ms during resting state and Judah, Shurkova, Hager, White, Taylor and Grant (93) selected HEP from electrode *Fz* averaged over 200 to 350 ms. Resting conditions have been associated with low interoceptive intensity, which increased difficulty to identify individual differences of cardiac interoception, so increasing sympathetic activity by tasks, such as negative emotion processing in our study, may facilitate cardiac interoception (94). Furthermore, as shown in Figure 3, the HEP cluster negatively correlated to BDI in UU conditions was located in the occipital, left temporoparietal, and left lateral frontal regions. HEP amplitudes over electrodes at left temporal and lateral frontal regions have been suggested as the afferent cortical representation of myocardial function (95). From a predictive coding perspective, sensitivity on interoceptive signals may be tied to efficient predictive coding processing.

The weak anticipatory HEP in high BDI individuals may result from reduced attention to cardiac signals and enhanced attention to incoming external events. HEP amplitude appeared to be enhanced when participants attended to heartbeats, comparing to external stimuli (96). The amplitude of HEP is considered a neural correlate of prediction processing (97, 98). In the model proposed by Barrett, Quigley and Hamilton (23), depression may be associated with inefficiency of prediction model, including low precision of predictive signals and/or deviated prior belief (99, 100). Precision, or the inverse of uncertainty, is built on the reliability of environment and modulated by attention (8, 96, 101). Precision is predicted in the high hierarchy and is top-down signaled to low-level areas that determine which prediction errors merit attention (102, 103). Enhanced attention to a specific signal can increase the precision. It has

been shown that depressive trait may relate to *reduced* precision in prediction and *increased* precision in prediction error (100). Therefore, our results imply that HDR is associated with 'reduced precision' or 'deviated prior belief' for interoceptive prediction, which may emerge from discrepancies between prediction and prediction error for a long time in the lives of HDR individuals (100).

Effects of certainty on the temporoparietal HEP cluster were enlarged with BDI scores (Figure 4c). In the other words, interoceptive signals around this region reflecting certainty levels, or predictions, enlarged with heightening depression risk. It has been reported that HDR individuals may have altered anticipatory responses in the INS, ventrolateral PFC, ACC, and ventral striatum (35, 36). The INS is considered as one of major neural sources underlying HEP (104), and is responsible for processing prediction and prediction error of current and future physiological status (29, 32). Thus, our findings provide additional neurophysiological evidence for alterations associated with depression risk in cardiac interoception. Further investigation on the cortical sources of left temporoparietal HEP may clarify if associations between anticipatory HEP and depression risk depend on distinct interoceptive brain regions.

Our post hoc analysis for HR time series confirmed earlier findings that pictures of negative valence *decelerated* HR more than those of positive valence (6, 105-107). Some studies reported larger deceleration of HR for unpredictable stimuli than for predictable ones (31, 32). Instead, we found the opposite trend, that HR deceleration in response to unpredictable pictures was smaller than to predictable pictures (Figure 1b). This may result from different durations of baseline correction (46). Various previous studies used the period before the presentation of pictures as baseline. Since anticipation induces changes of physiological activity (108, 109), our design may be more sensitive to effects of anticipation. Thus, we provide evidence that modulation of cardiac activity initiates during the anticipation stage, suggesting that research on physiological activity should consider effects of anticipation, if various predictive cues are applied.

Our analysis for HRV time series was in line with the previous literature that HRV in response to positive valence was higher than to negative valence (110). In contrast, another study reported reduced HRV after display of emotional pictures (12). Differences may cause by signal processing method and experiment paradigm. In the experiment of MacKinnon, Gevirtz, McCraty and Brown (12), positive or negative affect was induced via 5 minutes of speeches. Thus, the cardiac regulation may be different between long-term

and short-term changes or between responses to mood and emotion. Furthermore, our paired t-test analysis showed the effect of certainty on HRV in positive emotion conditions while the alternation of certainty effects with BDI were found in negative emotion conditions (Figure 2d). It suggests that prediction error signals elicited by unexpected negative emotion is altered by depression risk. Additionally, the correlation between certainty effects of HEP and BDI in negative conditions (Figure 4c) may indicate that the neural processing of prediction is modulated by depression risk. Unfortunately, no significant correlation was found between the neural signals forming predictions and cardiac signals forming prediction errors (Figure 5d) and their relationship was not mediated by BDI scores (Figure 5c). It may be explained by nonlinear relationships for predictive coding between HEP and HRV. Future studies based on other types of neural and cardiac indices and using computational models (111, 112) may be needed to examine predictive coding in neuro-cardiac interactions.

We also examined temporal characteristics of HR and HRV changes for anticipation based on predictive cues and perception of emotional pictures. The effects of certainty on HR appeared from 0.7 s and differential deceleration of HR between emotional pictures appeared at around 5.4 s, followed by the recovery of HR after 10 to 12 s (Figure 1a). Cardiac activity was remotely controlled by central autonomic network (CNS) via the regulation of ANS (113). The two branches of ANS, parasympathetic (PNS) and sympathetic nervous systems (SNS), act antagonistically to regulate cardiac activity. It is well known that activation of PNS decreases HR, whereas activation of SNS increases HR. The PNS exerts its effect on cardiac signals after 1 s, while the SNS exerts its effect after 5 s (114). Thus, HR deceleration initiated during the cue phase may be modulated mainly by activated PNS and the recovery of HR may reflect the activation of the SNS. As to HRV, the responses increased after display of cues and reached peaks at around 9 to 10 s. SDNN, the measures of HRV in this study, is contributed from activity of both SNS and PNS (114). Altogether, the effects of PNS and SNS reduced around 10 seconds after displays of cues, or around 6 seconds after display of pictures. Moreover, the largely decreased HR and increased SDNN in the UU condition may indicate exaggerated PNS activity elicited by unexpected negative stimuli among HDR individuals.

Despite our comprehensive analyses, this study has several limitations. First, since it was not feasible for our event-related paradigm and because it has been suggested that accurate measures of SDNN can be

obtained from 10-s ECG recordings (115, 116), we computed temporal dynamics of HRV using a 10-s sliding window. Our analysis of HRV may not be directly comparable to the standard short-term HRV from 5-min ECG recordings (47). Second, our analysis of cardiac reactivity was limited to two time-domain parameters, HR and SDNN. As cardiac reactivity markers for HRV, frequency-domain parameters, such as low- or high-frequency components or non-linear geometric method (114) might be possible. However, these measures typically require ECG recordings of at least 60 s are necessary (115), so they would not fit well with our experimental design. Therefore, future studies could assess this using different experimental designs, such as a blocked design with longer inter-trial-interval rather than the event-related design we employed here. Third, although we tried to dissociate event-related effects of cue and picture on cardiac reactivity, temporal dissociation might not be perfectly achievable because of the fixed time interval between cues and pictures in our paradigm. Further investigations would be required to disentangle the temporal characterization of these effects. Although limitations and discrepancies exit in this study, our evidence supports the notion that HDR affects interoceptive cardiac processing responding to cues and emotional pictures.

To conclude, our findings reveal that HDR was associated with excessive cardiac reactivity, reduced anticipatory HEP, and enhanced neuro-cardio interactions to unexpected negative stimuli. It may account for overactive PNS, reduced BRS, and ineffective interoceptive predictive coding. These findings suggest alternations in ANS and cardiac interoceptive system as well as their inter-relation may reflect depression risk. The marker may have potential for neurophysiological feedback treatment for depressive population. Our findings extend understanding of emotional processing under certainty and uncertainty in healthy populations and a novel link between depression risk and brain-heart interactions were identified through detailed characterization of cardiac reactivity and HEP time series.

References

1. **Kuppens P, and Verduyn P**. Emotion dynamics. *Current Opinion in Psychology* 17: 22-26, 2017.
2. **Critchley HD, and Garfinkel SN**. Interoception and emotion. *Current Opinion in Psychology* 17: 7-14, 2017.
3. **Eggart M, Lange A, Binser MJ, Queri S, and Müller-Oerlinghausen B**. Major depressive disorder is associated with impaired interoceptive accuracy: a systematic review. *Brain Sciences* 9: 131, 2019.
4. **Avery JA, Drevets WC, Moseman SE, Bodurka J, Barcalow JC, and Simmons WK**. Major depressive disorder is associated with abnormal interoceptive activity and functional connectivity in the insula. *Biological Psychiatry* 76: 258-266, 2014.
5. **Stuhrmann A, Suslow T, and Dannlowski U**. Facial emotion processing in major depression: a systematic review of neuroimaging findings. *Biology of Mood & Anxiety Disorders* 1: 10, 2011.
6. **Ilves M, and Surakka V**. Heart rate responses to synthesized affective spoken words. *Advances in Human-Computer Interaction* 2012: 158487, 2012.
7. **Kop WJ, Synowski SJ, Newell ME, Schmidt LA, Waldstein SR, and Fox NA**. Autonomic nervous system reactivity to positive and negative mood induction: The role of acute psychological responses and frontal electrocortical activity. *Biological Psychology* 86: 230-238, 2011.
8. **Coll M-P, Hobson H, Bird G, and Murphy J**. Systematic review and meta-analysis of the relationship between the heartbeat-evoked potential and interoception. *Neuroscience & Biobehavioral Reviews* 122: 190-200, 2021.
9. **Salamone PC, Sedeño L, Legaz A, Bekinschtein T, Martorell M, Adolfi F, Fraile-Vazquez M, Rodríguez Arriagada N, Favaloro L, Peradejordi M, Absi DO, García AM, Favaloro R, and Ibáñez A**. Dynamic neurocognitive changes in interoception after heart transplant. *Brain Communications* 2: fcaa095, 2020.
10. **Ravijts L**. Revealing temporal interactions around the heartbeat-evoked potential modulated by emotional perception. Ghent University, 2019.
11. **Valenza G, Greco A, Gentili C, Lanata A, Sebastiani L, Menicucci D, Gemignani A, Scilingo EP.** Combining electroencephalographic activity and instantaneous heart rate for assessing brain-heart dynamics during visual emotional elicitation in healthy subjects. *Philosophical Transactions of the Royal Society A: Mathematical, Physical and Engineering Sciences* 374:20150176, 2016.
12. **MacKinnon S, Gevirtz R, McCraty R, and Brown M**. Utilizing Heartbeat Evoked Potentials to Identify Cardiac Regulation of Vagal Afferents During Emotion and Resonant Breathing. *Applied Psychophysiology and Biofeedback* 38: 241-255, 2013.
13. **Strigo IA, Matthews SC, and Simmons AN**. Right anterior insula hypoactivity during anticipation of homeostatic shifts in major depressive disorder. *Psychosomatic Medicine* 72: 2010.
14. **Fergusson DM, Horwood LJ, Ridder EM, and Beautrais AL**. Subthreshold depression in adolescence and mental health outcomes in adulthood. *Archives of General Psychiatry* 62: 66-72, 2005.
15. **Hwang JW, Egorova N, Yang XQ, Zhang WY, Chen J, Yang XY, Hu LJ, Sun S, Tu Y, and Kong J**. Subthreshold depression is associated with impaired resting-state functional connectivity of the cognitive control network. *Translational Psychiatry* 5: e683, 2015.
16. **Peng X, Lau WKW, Wang C, Ning L, and Zhang R**. Impaired left amygdala resting state functional connectivity in subthreshold depression individuals. *Scientific Reports* 10: 17207, 2020.
17. **Terhaar J, Viola FC, Bär K-J, and Debener S**. Heartbeat evoked potentials mirror altered body perception in depressed patients. *Clinical Neurophysiology* 123: 1950-1957, 2012.
18. **Damasio A, and Carvalho GB**. The nature of feelings: evolutionary and neurobiological origins. *Nature Reviews Neuroscience* 14: 143-152, 2013.
19. **Pinna T, and Edwards DJ**. A systematic review of associations between interoception, vagal tone, and emotional regulation: potential applications for mental health, wellbeing, psychological flexibility, and chronic conditions. *Frontiers in psychology* 11: 1792-1792, 2020.
20. **Leopold C, and Schandry R**. The heartbeat-evoked brain potential in patients suffering from diabetic neuropathy and in healthy control persons. *Clinical Neurophysiology* 112: 674-682, 2001.
21. **De Zorzi L, Ranfaing S, Honoré J, and Sequeira H**. Autonomic reactivity to emotion: A marker of sub-clinical anxiety and depression symptoms? *Psychophysiology* 58: e13774, 2021.
22. **Dell'Acqua C, Dal Bò E, Messerotti Benvenuti S, and Palomba D**. Reduced heart rate variability is associated with vulnerability to depression. *Journal of Affective Disorders Reports* 1: 100006, 2020.
23. **Barrett LF, Quigley KS, and Hamilton P**. An active inference theory of allostasis and interoception in depression. *Philosophical Transactions of the Royal Society B: Biological Sciences* 371: 20160011, 2016.
24. **Seth A, Suzuki K, and Critchley H**. An interoceptive predictive coding model of conscious presence. *Frontiers in Psychology* 2: 395, 2012.

25. **Friston K, and Kiebel S**. Predictive coding under the free-energy principle. *Philosophical transactions of the Royal Society of London Series B, Biological sciences* 364: 1211-1221, 2009.
26. **Friston K**. The free-energy principle: A unified brain theory? *Nature Reviews Neuroscience* 11: 127-138, 2010.
27. **Sterling P**. Allostasis: A model of predictive regulation. *Physiology & Behavior* 106: 5-15, 2012.
28. **Kok P, Bains Lauren J, van Mourik T, Norris David G, and de Lange Floris P**. Selective activation of the deep layers of the human primary visual cortex by top-down feedback. *Current Biology* 26: 371-376, 2016.
29. **Livneh Y, Sugden AU, Madara JC, Essner RA, Flores VI, Sugden LA, Resch JM, Lowell BB, and Andermann ML**. Estimation of current and future physiological states in insular cortex. *Neuron* 105: 1094-1111.e1010, 2020.
30. **Corcoran AW, Macefield VG, and Hohwy J**. Be still my heart: Cardiac regulation as a mode of uncertainty reduction. *Psychonomic Bulletin & Review* 28: 1211-1223, 2021.
31. **Murakami H, Matsunaga M, and Ohira H**. Phasic heart rate responses for anticipated threat situations. *International Journal of Psychophysiology* 77: 21-25, 2010.
32. **Tracy LM, Gibson SJ, Georgiou-Karistianis N, and Giummarra MJ**. Effects of explicit cueing and ambiguity on the anticipation and experience of a painful thermal stimulus. *PLOS ONE* 12: e0183650, 2017.
33. **Gentsch A, Sel A, Marshall AC, and Schütz-Bosbach S**. Affective interoceptive inference: Evidence from heart-beat evoked brain potentials. *Human Brain Mapping* 40: 20-33, 2019.
34. **Marshall AC, Gentsch A, Jelinčić V, and Schütz-Bosbach S**. Exteroceptive expectations modulate interoceptive processing: repetition-suppression effects for visual and heartbeat evoked potentials. *Scientific Reports* 7: 16525, 2017.
35. **Argyris Stringaris, M.D., Ph.D. ,, Pablo Vidal-Ribas Belil, M.Sc. ,, Eric Artiges, M.D., Ph.D. ,, Hervé Lemaitre, Ph.D. ,, Fanny Gollier-Briant, M.D., Ph.D. ,, Selina Wolke, M.Sc. ,, Hélène Vulser, M.D. ,, Ruben Miranda, M.Psych. ,, Jani Penttilä, M.D., Ph.D. ,, Maren Struve, Ph.D. ,, Tahmine Fadai, M.D. ,, Viola Kappel, Dipl.-Psych. ,, Yvonne Grimmer, M.D. ,, Robert Goodman, Ph.D., F.R.C.Psych. ,, Luise Poustka, M.D. ,, Patricia Conrod, Ph.D. ,, Anna Cattrell, Ph.D. ,, Tobias Banaschewski, M.D., Ph.D. ,, Arun L.W. Bokde, Ph.D. ,, Uli Bromberg, M.D. ,, Christian Büchel, M.D. ,, Herta Flor, Ph.D. ,, Vincent Frouin, Ph.D. ,, Juergen Gallinat, M.D. ,, Hugh Garavan, Ph.D. ,, Penny Gowland, Ph.D. ,, Andreas Heinz, M.D. ,, Bernd Ittermann, Ph.D. ,, Frauke Nees, Ph.D. ,, Dimitri Papadopoulos, Ph.D. ,, Tomas Paus, M.D., Ph.D. ,, Michael N. Smolka, M.D. ,, Henrik Walter, M.D., Ph.D. ,, Rob Whelan, Ph.D. ,, Jean-Luc Martinot, M.D., Ph.D. ,, Gunter Schumann, M.D. ,, and Marie-Laure Paillère-Martinot, M.D., Ph.D. ,**. The brain's response to reward anticipation and depression in adolescence: Dimensionality, specificity, and longitudinal predictions in a community-based sample. *American Journal of Psychiatry* 172: 1215-1223, 2015.
36. **He Z, Zhang D, Muhlert N, and Elliott R**. Neural substrates for anticipation and consumption of social and monetary incentives in depression. *Social Cognitive and Affective Neuroscience* 14: 815-826, 2019.
37. **Machizawa MG, Lisi G, Kanayama N, Mizuochi R, Makita K, Sasaoka T, and Yamawaki S**. Quantification of anticipation of excitement with a three-axial model of emotion with EEG. *Journal of Neural Engineering* 17: 036011, 2020.
38. **Beck AT, Steer RA, and Brown G**. Beck depression inventory–II. *Psychological Assessment* 1996.
39. **Spielberger CD, Ritterband LM, Reheiser EC, and Brunner TM**. The nature and measurement of depression. *International Journal of Clinical and Health Psychology* 3: 209-234, 2003.
40. **Preacher KJ, Rucker DD, MacCallum RC, and Nicewander WA**. Use of the extreme groups approach: A critical reexamination and new recommendations. *Psychological Methods* 10: 178-192, 2005.
41. **Grissom RJ, and Kim JJ**. *Effect sizes for research: univariate and multivariate applications*. New York: Taylor & Francis Group, 2011.
42. **Beatty S, and Hewitt J**. Affective reactions to failure as a function of effort and depression. *Perceptual and Motor Skills* 80: 33-34, 1995.
43. **Lang PJ, Bradley MM, and Cuthbert BN**. International affective picture system (IAPS): Technical manual and affective ratings. 1: 39-58, 1997.
44. **Carreiras C, Alves AP, Lourenço A, Canento F, Silva H, and Fred A**. BioSPPy - Biosignal Processing in Python https://github.com/PIA-Group/BioSPPy/
45. **Hamilton P**. Open source ECG analysis. In: *Computers in Cardiology*2002, p. 101-104.
46. **Jennings JR, Berg WK, Hutcheson JS, Obrist P, Porges S, and Turpin G**. Committee report. Publication guidelines for heart rate studies in man. *Psychophysiology* 18: 226-231, 1981.
47. **Task Force of the European Society of Cardiology the North American Society of Pacing Electrophysiology**. Heart Rate Variability. *Circulation* 93: 1043-1065, 1996.

48. **Berntson GG, Thomas Bigger JR. J, Eckberg DL, Grossman P, Kaufmann PG, Malik M, Nagaraja HN, Porges SW, Saul JP, Stone PH, and Van der Molen MW**. Heart rate variability: Origins, methods, and interpretive caveats. *Psychophysiology* 34: 623-648, 1997.
49. **Delorme A, and Makeig S**. EEGLAB: an open source toolbox for analysis of single-trial EEG dynamics including independent component analysis. *Journal of Neuroscience Methods* 134: 9-21, 2004.
50. **Gramfort A, Luessi M, Larson E, Engemann D, Strohmeier D, Brodbeck C, Goj R, Jas M, Brooks T, Parkkonen L, and Hämäläinen M**. MEG and EEG data analysis with MNE-Python. *Frontiers in Neuroscience* 7: 267, 2013.
51. **Vallat R**. Pingouin: statistics in Python. *Journal of Open Source Software* 3: 1026, 2018.
52. **Virtanen P, Gommers R, Oliphant TE, Haberland M, Reddy T, Cournapeau D, Burovski E, Peterson P, Weckesser W, Bright J, van der Walt SJ, Brett M, Wilson J, Millman KJ, Mayorov N, Nelson ARJ, Jones E, Kern R, Larson E, Carey CJ, Polat İ, Feng Y, Moore EW, VanderPlas J, Laxalde D, Perktold J, Cimrman R, Henriksen I, Quintero EA, Harris CR, Archibald AM, Ribeiro AH, Pedregosa F, van Mulbregt P, Vijaykumar A, Bardelli AP, Rothberg A, Hilboll A, Kloeckner A, Scopatz A, Lee A, Rokem A, Woods CN, Fulton C, Masson C, Häggström C, Fitzgerald C, Nicholson DA, Hagen DR, Pasechnik DV, Olivetti E, Martin E, Wieser E, Silva F, Lenders F, Wilhelm F, Young G, Price GA, Ingold G-L, Allen GE, Lee GR, Audren H, Probst I, Dietrich JP, Silterra J, Webber JT, Slavič J, Nothman J, Buchner J, Kulick J, Schönberger JL, de Miranda Cardoso JV, Reimer J, Harrington J, Rodríguez JLC, Nunez-Iglesias J, Kuczynski J, Tritz K, Thoma M, Newville M, Kümmerer M, Bolingbroke M, Tartre M, Pak M, Smith NJ, Nowaczyk N, Shebanov N, Pavlyk O, Brodtkorb PA, Lee P, McGibbon RT, Feldbauer R, Lewis S, Tygier S, Sievert S, Vigna S, Peterson S, More S, Pudlik T, Oshima T, Pingel TJ, Robitaille TP, Spura T, Jones TR, Cera T, Leslie T, Zito T, Krauss T, Upadhyay U, Halchenko YO, Vázquez-Baeza Y, and SciPy C**. SciPy 1.0: fundamental algorithms for scientific computing in Python. *Nature Methods* 17: 261-272, 2020.
53. **Seabold S, and Perktold J**. statsmodels: Econometric and statistical modeling with python. In: *9th Python in Science Conference*2010.
54. **Kret ME, and De Gelder B**. A review on sex differences in processing emotional signals. *Neuropsychologia* 50: 1211-1221, 2012.
55. **Lee SA, Kim C-Y, Shim M, and Lee S-H**. Gender differences in neural responses to perceptually invisible fearful face-an ERP Study. *Front Behav Neurosci* 11: 6-6, 2017.
56. **Li H, Yuan J, and Lin C**. The neural mechanism underlying the female advantage in identifying negative emotions: An event-related potential study. *NeuroImage* 40: 1921-1929, 2008.
57. **Lithari C, Frantzidis CA, Papadelis C, Vivas AB, Klados MA, Kourtidou-Papadeli C, Pappas C, Ioannides AA, and Bamidis PD**. Are females more responsive to emotional stimuli? a neurophysiological study across arousal and valence dimensions. *Brain Topography* 23: 27-40, 2010.
58. **Nashiro K, Sakaki M, and Mather M**. Age differences in brain activity during emotion processing: Reflections of age-related decline or increased emotion regulation. *Gerontology* 58: 156-163, 2012.
59. **Kamp S-M, Schulz A, Forester G, and Domes G**. Older adults show a higher heartbeat-evoked potential than young adults and a negative association with everyday metacognition. *Brain Research* 1752: 147238, 2021.
60. **Ryan SM, Goldberger AL, Pincus SM, Mietus J, and Lipsitz LA**. Gender- and age-related differences in heart rate dynamics: Are women more complex than men? *Journal of the American College of Cardiology* 24: 1700-1707, 1994.
61. **Hart J**. Association between heart rate variability and manual pulse rate. *J Can Chiropr Assoc* 57: 243-250, 2013.
62. **Kazmi SZH, Zhang H, Aziz W, Monfredi O, Abbas SA, Shah SA, Kazmi SSH, and Butt WH**. Inverse correlation between heart rate variability and heart rate demonstrated by linear and nonlinear analysis. *PLOS ONE* 11: e0157557, 2016.
63. **Machado AV, Pereira MG, Souza GGL, Xavier M, Aguiar C, de Oliveira L, and Mocaiber I**. Association between distinct coping styles and heart rate variability changes to an acute psychosocial stress task. *Scientific Reports* 11: 24025, 2021.
64. **Choi K-H, Kim J, Kwon OS, Kim MJ, Ryu YH, and Park J-E**. Is heart rate variability (HRV) an adequate tool for evaluating human emotions? – A focus on the use of the International Affective Picture System (IAPS). *Psychiatry Research* 251: 192-196, 2017.
65. **Gotlib IH, and Joormann J**. Cognition and depression: current status and future directions. *Annual Review of Clinical Psychology* 6: 285-312, 2010.
66. **Lin X-X, Sun Y-B, Wang Y-Z, Fan L, Wang X, Wang N, Luo F, and Wang J-Y**. Ambiguity processing bias induced by depressed mood is associated with diminished pleasantness. *Scientific Reports* 9: 18726, 2019.

67. **Hartmann R, Schmidt FM, Sander C, and Hegerl U**. Heart rate variability as indicator of clinical state in depression. *Frontiers in Psychiatry* 9: 2019.
68. **Rechlin T, Weis M, Spitzer A, and Kaschka WP**. Are affective disorders associated with alterations of heart rate variability? *Journal of Affective Disorders* 32: 271-275, 1994.
69. **Huang M, Shah A, Su S, Goldberg J, Lampert RJ, Levantsevych OM, Shallenberger L, Pimple P, Bremner JD, and Vaccarino V**. Association of depressive symptoms and heart rate variability in Vietnam war–era twins: a longitudinal twin difference study. *JAMA Psychiatry* 75: 705-712, 2018.
70. **Schultchen D, Schneider C, Berberich G, Zaudig M, Erle TM, and Pollatos O**. On the relationship of interoceptive accuracy and attention: A controlled study with depressed inpatients and a healthy cohort. *Frontiers in Psychology* 11: 2021.
71. **Smith R, Feinstein JS, Kuplicki R, Forthman KL, Stewart JL, Paulus MP, Aupperle RL, Bodurka J, Savitz JB, Victor TA, Khalsa SS, and Tulsa I**. Perceptual insensitivity to the modulation of interoceptive signals in depression, anxiety, and substance use disorders. *Scientific Reports* 11: 2108, 2021.
72. **Burrows K, DeVille DC, Cosgrove KT, Kuplicki RT, Bodurka J, Guinjoan S, Savitz J, Victor TA, Paulus MP, Aupperle R, Khalsa SS, and Stewart JL**. Impact of serotonergic medication on interoception in major depressive disorder. *Biological Psychology* 169: 108286, 2022.
73. **Jandackova VK, Britton A, Malik M, and Steptoe A**. Heart rate variability and depressive symptoms: a cross-lagged analysis over a 10-year period in the Whitehall II study. *Psychological Medicine* 46: 2121-2131, 2016.
74. **Bohman H, Jonsson U, Päären A, von Knorring L, Olsson G, and von Knorring A-L**. Prognostic significance of functional somatic symptoms in adolescence: a 15-year community-based follow-up study of adolescents with depression compared with healthy peers. *BMC Psychiatry* 12: 90, 2012.
75. **Nakao M, and Yano E**. Somatic symptoms for predicting depression: One-year follow-up study in annual health examinations. *Psychiatry and Clinical Neurosciences* 60: 219-225, 2006.
76. **Lampert R, Bremner JD, Su S, Miller A, Lee F, Cheema F, Goldberg J, and Vaccarino V**. Decreased heart rate variability is associated with higher levels of inflammation in middle-aged men. *American Heart Journal* 156: 759.e751-759.e757, 2008.
77. **Imai J, and Katagiri H**. Regulation of systemic metabolism by the autonomic nervous system consisting of afferent and efferent innervation. *International Immunology* 34: 67-79, 2022.
78. **Gilbert JR, Wusinich C, and Zarate CA, Jr.** A predictive coding framework for understanding major depression. *Frontiers in human neuroscience* 16: 787495-787495, 2022.
79. **Catrambone V, Messerotti Benvenuti S, Gentili C, and Valenza G**. Intensification of functional neural control on heartbeat dynamics in subclinical depression. *Translational Psychiatry* 11: 221, 2021.
80. **Broadley AJM, Frenneaux MP, Moskvina V, Jones CJH, and Korszun A**. Baroreflex sensitivity Is reduced in depression. *Psychosomatic Medicine* 67: 2005.
81. **Davydov DM, Shapiro D, Cook IA, and Goldstein I**. Baroreflex mechanisms in major depression. *Progress in Neuro-Psychopharmacology and Biological Psychiatry* 31: 164-177, 2007.
82. **Bonyhay I, Risk M, and Freeman R**. High-pass filter characteristics of the baroreflex – a comparison of frequency domain and pharmacological methods. *PLOS ONE* 8: e79513, 2013.
83. **Suarez-Roca H, Mamoun N, Sigurdson MI, and Maixner W**. Baroreceptor modulation of the cardiovascular system, pain, consciousness, and cognition. In: *Compr Physiol*2021, p. 1373-1423.
84. **Minati L, Jones CL, Gray MA, Medford N, Harrison NA, and Critchley HD**. Emotional modulation of visual cortex activity: a functional near-infrared spectroscopy study. *Neuroreport* 20: 1344-1350, 2009.
85. **Okon-Singer H, Mehnert J, Hoyer J, Hellrung L, Schaare HL, Dukart J, and Villringer A**. Neural control of vascular reactions: Impact of emotion and attention. *The Journal of Neuroscience* 34: 4251-4259, 2014.
86. **Sible IJ, Jang JY, Sultzer DL, and Nation DA**. Visit-to-visit blood pressure variability and subthreshold depressive symptoms in older adults. *The American Journal of Geriatric Psychiatry* 2022.
87. **Iellamo F, Manzi V, Caminiti G, Sposato B, Massaro M, Cerrito A, Rosano G, and Volterrani M**. Dose-response relationship of baroreflex sensitivity and heart rate variability to individually-tailored exercise training in patients with heart failure. *International Journal of Cardiology* 166: 334-339, 2013.
88. **Iellamo F, Legramante JM, Massaro M, Raimondi G, and Galante A**. Effects of a residential exercise training on baroreflex sensitivity and heart rate variability in patients with coronary artery disease. *Circulation* 102: 2588-2592, 2000.
89. **Laterza MC, Matos LDNJd, Trombetta IC, Braga AMW, Roveda F, Alves MJNN, Krieger EM, Negrão CE, and Rondon MUPB**. Exercise training restores baroreflex sensitivity in never-treated hypertensive patients. *Hypertension* 49: 1298-1306, 2007.
90. **Mameletzi D, Kouidi E, Koutlianos N, and Deligiannis A**. Effects of long-term exercise training on cardiac baroreflex sensitivity in patients with coronary artery disease: a randomized controlled trial. *Clinical Rehabilitation* 25: 217-227, 2011.

91. **Lavie CJ, Milani RV, Cassidy MM, and Gilliland YE**. Effects of cardiac rehabilitation and exercise training programs in women with depression. *American Journal of Cardiology* 83: 1480-1483, 1999.
92. **Rutledge T, Redwine LS, Linke SE, and Mills PJ**. A meta-analysis of mental health treatments and cardiac rehabilitation for improving clinical outcomes and depression among patients with coronary heart disease. *Psychosomatic Medicine* 75: 2013.
93. **Judah MR, Shurkova EY, Hager NM, White EJ, Taylor DL, and Grant DM**. The relationship between social anxiety and heartbeat evoked potential amplitude. *Biological Psychology* 139: 1-7, 2018.
94. **Shivkumar K, Ajijola OA, Anand I, Armour JA, Chen P-S, Esler M, De Ferrari GM, Fishbein MC, Goldberger JJ, Harper RM, Joyner MJ, Khalsa SS, Kumar R, Lane R, Mahajan A, Po S, Schwartz PJ, Somers VK, Valderrabano M, Vaseghi M, and Zipes DP**. Clinical neurocardiology defining the value of neuroscience-based cardiovascular therapeutics. *The Journal of Physiology* 594: 3911-3954, 2016.
95. **Gray MA, Taggart P, Sutton PM, Groves D, Holdright DR, Bradbury D, Brull D, and Critchley HD**. A cortical potential reflecting cardiac function. *Proceedings of the National Academy of Sciences* 104: 6818-6823, 2007.
96. **Petzschner FH, Weber LA, Wellstein KV, Paolini G, Do CT, and Stephan KE**. Focus of attention modulates the heartbeat evoked potential. *NeuroImage* 186: 595-606, 2019.
97. **Pfeiffer C, and De Lucia M**. Cardio-audio synchronization drives neural surprise response. *Scientific Reports* 7: 14842, 2017.
98. **Ainley V, Apps MAJ, Fotopoulou A, and Tsakiris M**. 'Bodily precision': A predictive coding account of individual differences in interoceptive accuracy. *Philosophical Transactions of the Royal Society B: Biological Sciences* 371: 2016.
99. **Edwards MJ, Adams RA, Brown H, Pareés I, and Friston KJ**. A Bayesian account of 'hysteria'. *Brain* 135: 3495-3512, 2012.
100. **Badcock PB, Davey CG, Whittle S, Allen NB, and Friston KJ**. The depressed brain: An evolutionary systems theory. *Trends in Cognitive Sciences* 21: 182-194, 2017.
101. **Park H-D, and Blanke O**. Heartbeat-evoked cortical responses: Underlying mechanisms, functional roles, and methodological considerations. *NeuroImage* 197: 502-511, 2019.
102. **Barrett LF**. The theory of constructed emotion: an active inference account of interoception and categorization. *Social Cognitive and Affective Neuroscience* 12: 1-1, 2017.
103. **Feldman H, and Friston KJ**. Attention, uncertainty, and free-energy. *Frontiers in Human Neuroscience* 4: 2010.
104. **Park H-D, Bernasconi F, Salomon R, Tallon-Baudry C, Spinelli L, Seeck M, Schaller K, and Blanke O**. Neural sources and underlying mechanisms of neural responses to heartbeats, and their role in bodily self-consciousness: An intracranial EEG study. *Cerebral Cortex* 28: 2351-2364, 2017.
105. **Bradley MM, Miccoli L, Escrig MA, and Lang PJ**. The pupil as a measure of emotional arousal and autonomic activation. *Psychophysiology* 45: 602-607, 2008.
106. **Brouwer A-M, van Wouwe N, Mühl C, van Erp J, and Toet A**. Perceiving blocks of emotional pictures and sounds: effects on physiological variables. *Frontiers in human neuroscience* 7: 295-295, 2013.
107. **Pollatos O, Herbert BM, Matthias E, and Schandry R**. Heart rate response after emotional picture presentation is modulated by interoceptive awareness. *International Journal of Psychophysiology* 63: 117-124, 2007.
108. **Pastor MC, Poy R, Segarra P, and Moltó J**. Emotional reactivity during anticipation and perception of affective pictures. *The Spanish Journal of Psychology* 17: E110, 2014.
109. **Pulopulos MM, Vanderhasselt M-A, and De Raedt R**. Association between changes in heart rate variability during the anticipation of a stressful situation and the stress-induced cortisol response. *Psychoneuroendocrinology* 94: 63-71, 2018.
110. **Shi H, Yang L, Zhao L, Su Z, Mao X, Zhang L, and Liu C**. Differences of heart rate variability between happiness and sadness emotion states: A pilot study. *Journal of Medical and Biological Engineering* 37: 527-539, 2017.
111. **Allen M, Levy A, Parr T, and Friston KJ**. In the body's eye: the computational anatomy of interoceptive inference. *bioRxiv* 603928, 2019.
112. **Smith R, Mayeli A, Taylor S, Al Zoubi O, Naegele J, and Khalsa SS**. Gut inference: A computational modelling approach. *Biological Psychology* 164: 108152, 2021.
113. **Benarroch EE**. The central autonomic network: functional organization, dysfunction, and perspective. *Mayo Clinic Proceedings* 68: 988-1001, 1993.
114. **Shaffer F, and Ginsberg JP**. An Overview of Heart Rate Variability Metrics and Norms. *Front Public Health* 5: 258, 2017.
115. **Munoz ML, van Roon A, Riese H, Thio C, Oostenbroek E, Westrik I, de Geus EJC, Gansevoort R, Lefrandt J, Nolte IM, and Snieder H**. Validity of (Ultra-)Short Recordings for Heart Rate Variability Measurements. *PLOS ONE* 10: e0138921, 2015.

116. **van den Berg ME, Rijnbeek PR, Niemeijer MN, Hofman A, van Herpen G, Bots ML, Hillege H, Swenne CA, Eijgelsheim M, Stricker BH, and Kors JA**. Normal Values of Corrected Heart-Rate Variability in 10-Second Electrocardiograms for All Ages. *Frontiers in Physiology* 9: 424, 2018.

Acknowledgement

This study was supported by the Japan Science and Technology Agency (JST) COI (grant nos. JPMJCE1311 and JPMJCA2208), JST Moonshot Research and Development Program (grant no. JPMJMS2296) and the Grant-in-Aid for Early-Career Scientists (grant no. 20299115). We thank Noriaki Kanayama, at the National Institute of Advanced Industrial Science and Technology (AIST), Japan and Kai Makita at the University of Fukui, Japan, for data collection. CHL designed research, analyzed data and helped write the paper. MGM designed research and helped write the paper. RM analyzed data. SY obtained the research grant from the COI program, supervised research, and helped write the paper. The authors have no conflict of interest with regard to this research.

Figure Legends

Figure 1 Time series of (a) heart rate (HR) and (c) heart rate variability (HRV) and box plots of temporal averaged (b) HR and (d) HRV during time periods showing significant main effects. The gray-shaded area indicates the time period showing the significant main effect of emotional picture in the cue × pic RM-ANOVA analysis and horizontal lines represent the period showing a significant difference in paired *t*-tests ($p_{FDR} < .05$ and duration > 1 s). The left and right vertical dashed lines indicate the onsets of cue and picture presentation, respectively. Red and blue shaded areas along the HR and HRV time series represent one standard error. Red and blue colors represent predictable and unpredictable conditions, respectively. PP: predictable pleasant; PU: predictable unpleasant; UP: unpredictable pleasant; UU: unpredictable unpleasant.

Figure 2 Scatter plots (a) between BDI scores and HR changes under UU condition and (c) between BDI and certainty effect of HRV under unpleasant condition (PU-UU) and time series of (b) HR changes under UU condition and (c) HRV changes under PU and UU conditions in low BDI and high BDI groups. The black solid lines represent fitness lines for all samples. Cyan and magenta colors indicate high BDI and low BDI groups, respectively. Cyan- and magenta-shaded areas along the HR and HRV time series represent one standard error. In (b), the gray-shaded area represents the duration showing significance main effects of emotional pictures in RM-ANOVA analysis. In (d), the gray-shaded area represents the duration showing significant difference between PP and PU conditions. BDI: Beck Depression Index.

Figure 3 (a) Grand average of original heartbeat-evoked potential (HEP), obtained via epoching EEG signals based on actual R peaks, and surrogate HEP, obtained via epoching EEG signals based on randomly-shifted R peaks, during –0.1 to 0.6 s. The scalp distribution of HEP is viewed from above. (b) Blue squares, green triangles, and red circles indicate channel positions of HEP clusters 1, 2, and 3 determined by the spatiotemporal nonparametric cluster-level test over the time series of HEP and surrogate HEP during 0.1–0.6 s. Significant durations for HEP clusters 1, 2, and 3 are 0.10–0.36 s, 0.10–0.29 s, 0.29–0.33 s, respectively.

Figure 4 (a) Time series of averaged HEP across electrodes of cluster 1 in PU and UU conditions in cue phase and scatter plots of (b) BDI scores and HEP amplitude in cluster 1 under UU condition in cue phase and (c) BDI scores and certainty effects of HEP amplitude in cluster 1 under unpleasant conditions in cue phase. Gray-shaded areas indicate the duration of HEP cluster 1. Blue- and red-shaded areas along the HEP time series indicate one standard error. Dashed lines indicate the time of R peaks. Cyan and magenta colors indicate high BDI and low BDI groups, respectively.

Figure 5 Models to predict changes of heart rate (HR) under the unpredictable unpleasant (UU) condition from (a) the heartbeat evoked potential (HEP) of cluster 1 at *cue phase* and (c) the difference of HEP amplitude between PU and UU at cue phase (*PU – UU*) in cluster 1 mediated by depression risk, which is quantified using a BDI score. Scatter plots for (a) HEP amplitude and HR changes under the UU condition and for (d) certainty effects of HEP in cluster 1 at cue phase and HRV under unpleasant conditions. Cyan, magenta, and black solid lines represent regression lines fitted from high BDI group, low BDI group, and all participants. *: $p < .05$.

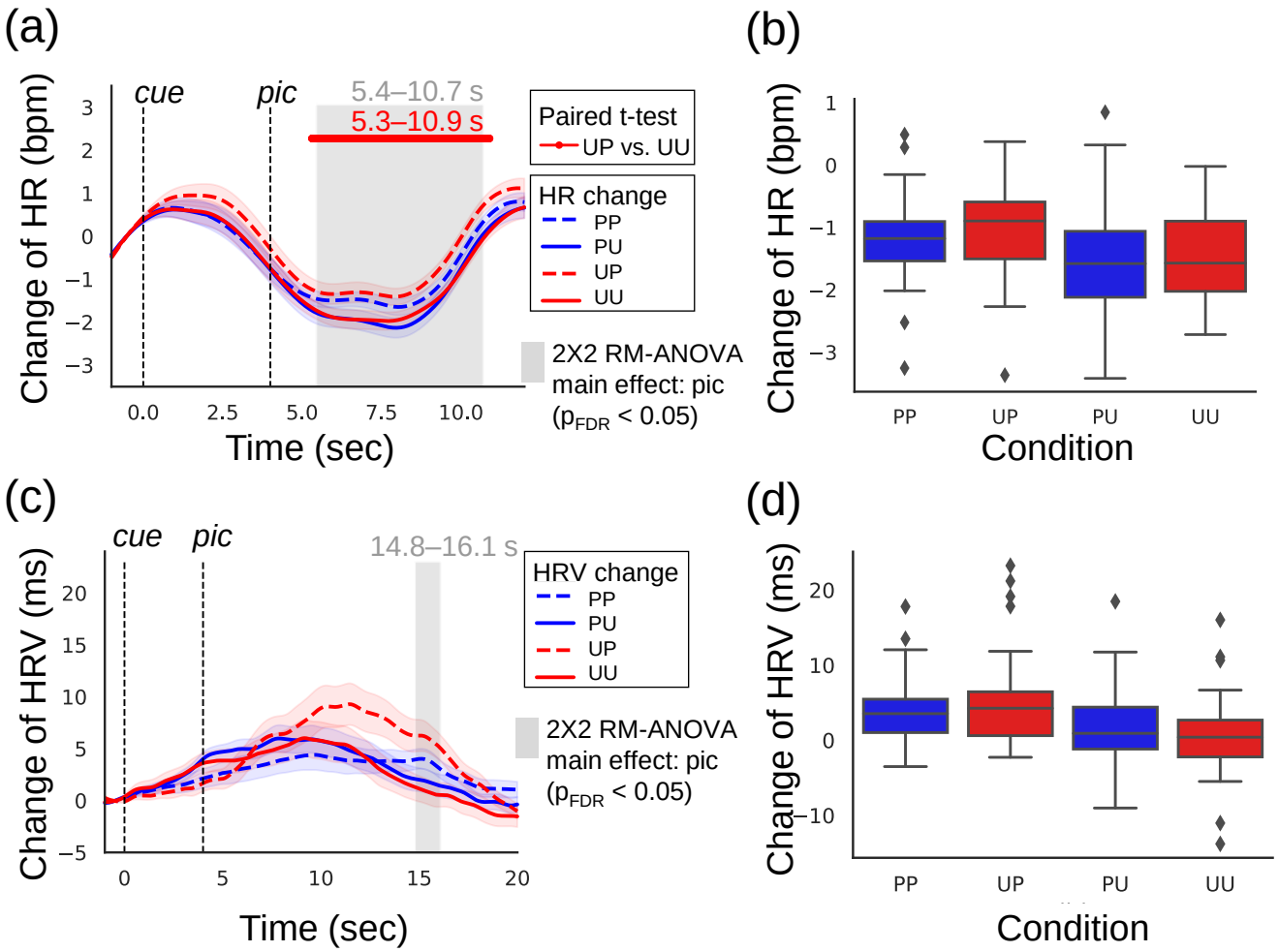
(a)
cue
pic
5.4–10.7 s
5.3–10.9 s
Paired t-test
UP vs. UU
HR change
PP
PU
UP
UU
2X2 RM-ANOVA
main effect: pic
(p_{FDR} < 0.05)
Change of HR (bpm)
Time (sec)
(b)
Change of HR (bpm)
PP
UP
PU
UU
Condition
(c)
cue
pic
14.8–16.1 s
HRV change
PP
PU
UP
UU
2X2 RM-ANOVA
main effect: pic
(p_{FDR} < 0.05)
Change of HRV (ms)
Time (sec)
(d)
Change of HRV (ms)
PP
UP
PU
UU
Condition

Figure 1

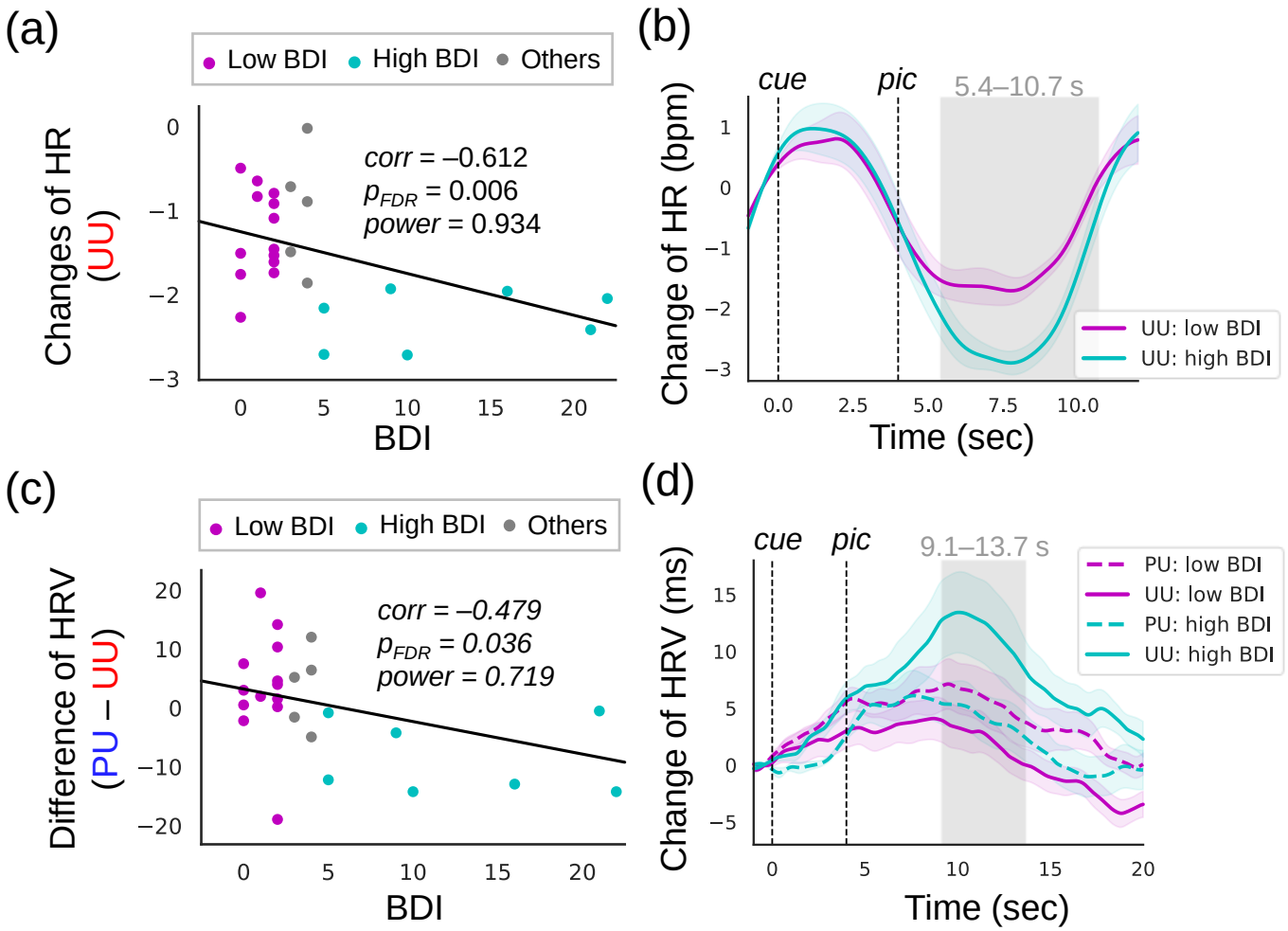
(a)
Low BDI
High BDI
Others
corr = –0.612
p_{FDR} = 0.006
power = 0.934
Changes of HR
(UU)
BDI
(b)
cue
pic
5.4–10.7 s
Change of HR (bpm)
Time (sec)
UU: low BDI
UU: high BDI
(c)
Low BDI
High BDI
Others
corr = –0.479
p_{FDR} = 0.036
power = 0.719
Difference of HRV
(PU – UU)
BDI
(d)
cue
pic
9.1–13.7 s
Change of HRV (ms)
Time (sec)
PU: low BDI
UU: low BDI
PU: high BDI
UU: high BDI

Figure 2

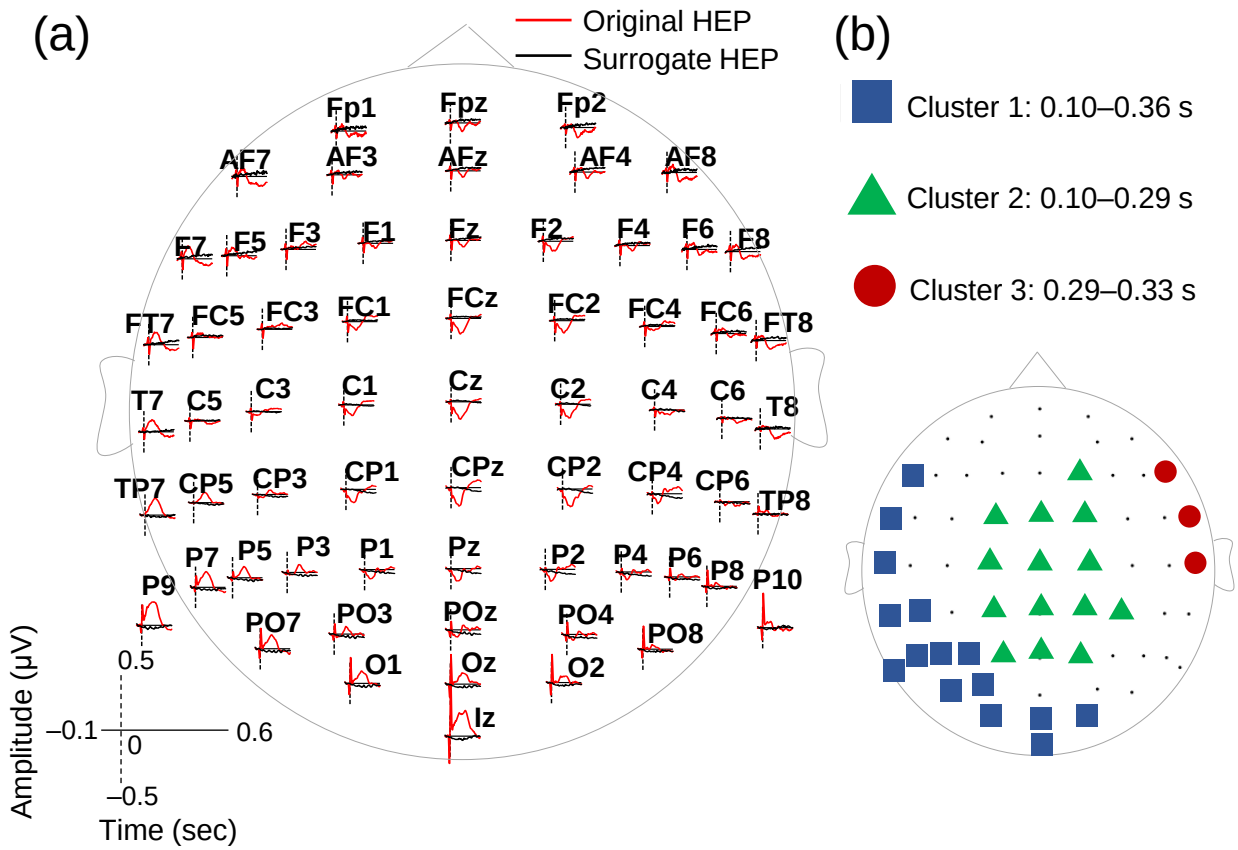
(a)
Original HEP
Surrogate HEP
Fp1
Fpz
Fp2
AF7
AF3
AFz
AF4
AF8
F7
F5
F3
F1
Fz
F2
F4
F6
F8
FT7
FC5
FC3
FC1
FCz
FC2
FC4
FC6
FT8
T7
C5
C3
C1
Cz
C2
C4
C6
T8
TP7
CP5
CP3
CP1
CPz
CP2
CP4
CP6
TP8
P9
P7
P5
P3
P1
Pz
P2
P4
P6
P8
P10
PO7
PO3
POz
PO4
PO8
O1
Oz
O2
Iz
0.5
–0.1
0
0.6
–0.5
Amplitude (μV)
Time (sec)
(b)
Cluster 1: 0.10–0.36 s
Cluster 2: 0.10–0.29 s
Cluster 3: 0.29–0.33 s

Figure 3

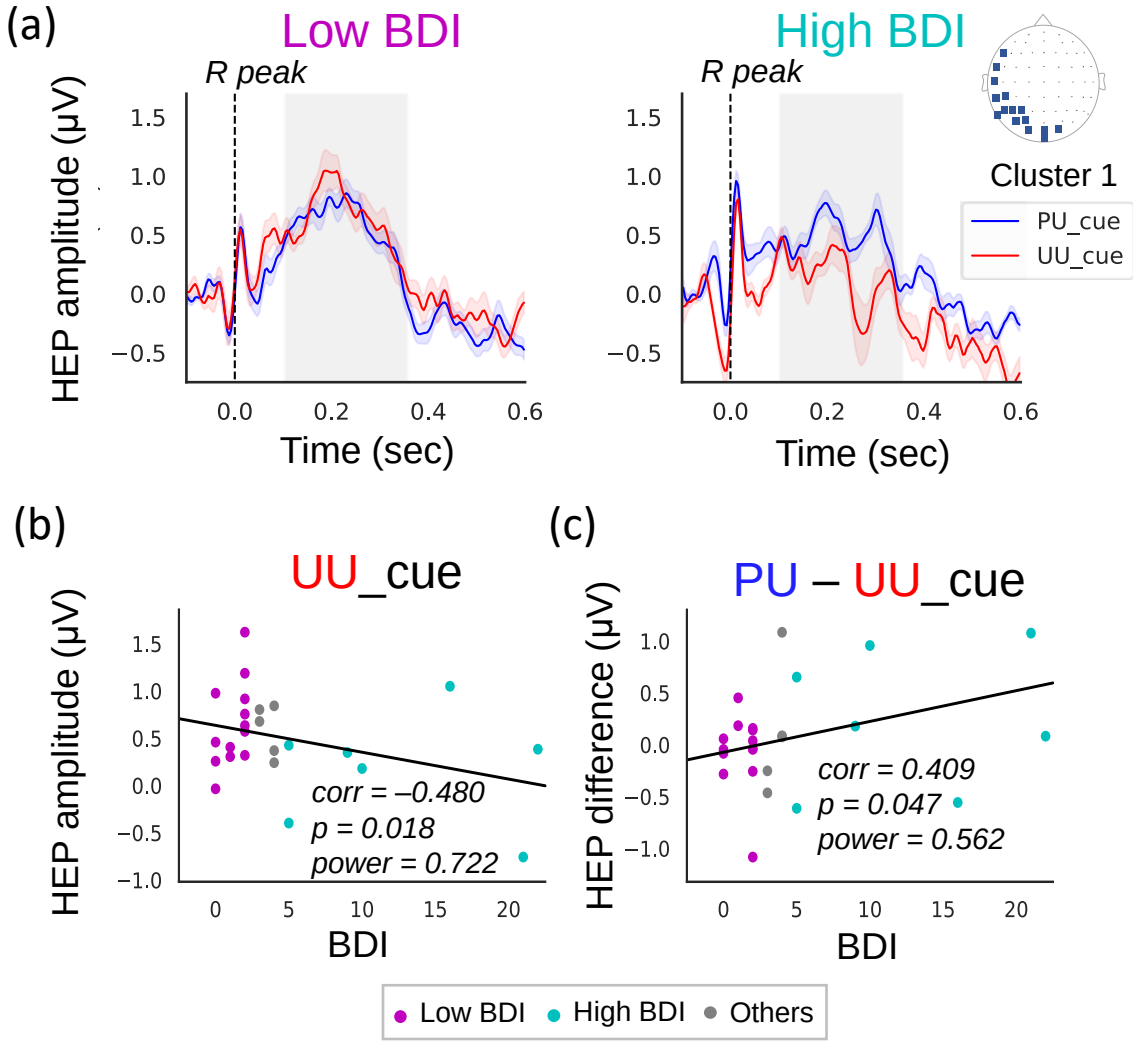
(a)
Low BDI
High BDI
R peak
R peak
HEP amplitude (μV)
Time (sec)
Time (sec)
Cluster 1
PU_cue
UU_cue
(b)
UU_cue
HEP amplitude (μV)
corr = –0.480
p = 0.018
power = 0.722
BDI
(c)
PU – UU_cue
HEP difference (μV)
corr = 0.409
p = 0.047
power = 0.562
BDI
Low BDI
High BDI
Others

Figure 4

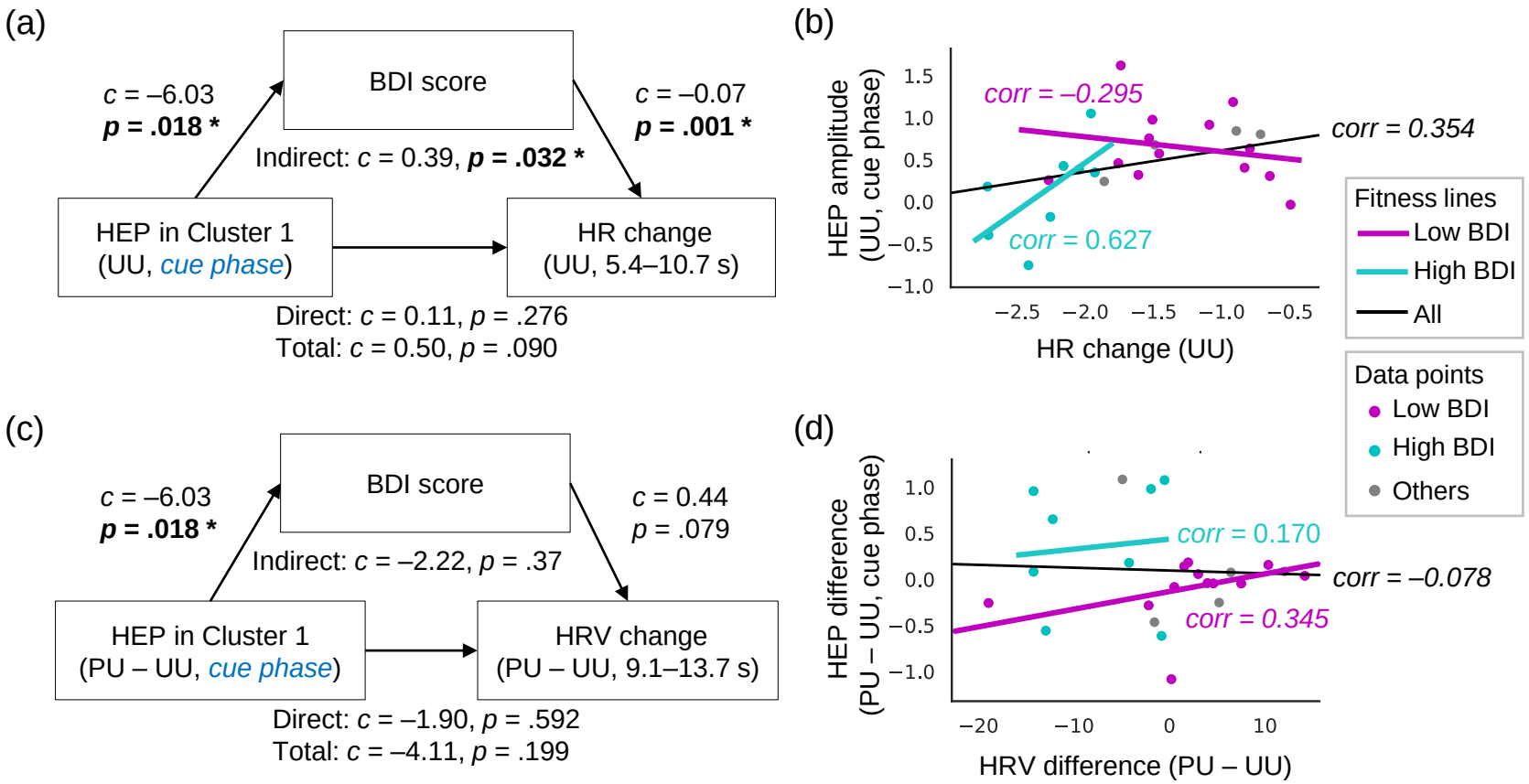
(a)
BDI score
c = –6.03
p = .018 *
c = –0.07
p = .001 *
Indirect: c = 0.39, p = .032 *
HEP in Cluster 1
(UU, cue phase)
HR change
(UU, 5.4–10.7 s)
Direct: c = 0.11, p = .276
Total: c = 0.50, p = .090
(b)
HEP amplitude
(UU, cue phase)
HR change (UU)
corr = –0.295
corr = 0.354
corr = 0.627
Fitness lines
Low BDI
High BDI
All
Data points
Low BDI
High BDI
Others
(c)
BDI score
c = –6.03
p = .018 *
c = 0.44
p = .079
Indirect: c = –2.22, p = .37
HEP in Cluster 1
(PU – UU, cue phase)
HRV change
(PU – UU, 9.1–13.7 s)
Direct: c = –1.90, p = .592
Total: c = –4.11, p = .199
(d)
HEP difference
(PU – UU, cue phase)
HRV difference (PU – UU)
corr = 0.170
corr = –0.078
corr = 0.345

Figure 5